JOURNAL OF GEOPHYSICAL RESEARCH, VOL. 90, NO. C5, PAGES 9137–9146, SEPTEMBER 20, 1985

Kinematic and Dynamic Estimates From Electromagnetic Current Meter Data

DAVID G. AUBREY

Woods Hole Oceanographic Institution, Massachusetts

JOHN H. TROWBRIDGE

University of Delaware, Newark

The dynamic response of electromagnetic current meters (manufactured by Marsh-McBirney, Inc.) has been clarified through a comprehensive laboratory measurement program combined with a thorough literature review. Elucidation of the behavior of these flow meters under a variety of dynamic conditions has been neglected in the past. Since flow past a spherical body has considerable hydrodynamic complexity for different dynamic conditions, a careful laboratory study was carried out for pure steady, pure oscillatory (horizontal plane), and combined steady/oscillatory conditions at two test facilities. Test results indicate that flow meter behavior under pure steady flow is reasonable in the absence of high levels of free-stream turbulence, with an rms error of 1–5 cm/s. These errors could be reduced with a higher-order polynomial regression fit. Pure oscillatory response was also reasonable, with rms errors of 1–2 cm/s, and sensitivity which is correlated with the oscillatory Reynolds number $(Re)_0$, and the Keulegan-Carpenter number (A/d, where A is the oscillation excursion and d is the probe diameter). Combined steady/oscillatory flows degraded current meter performance with larger residual errors (1–6 cm/s) and significant differences in sensitivity (up to 20%). Horizontal cosine response showed systematic deviations from pure cosine behavior, with a notable intercardinal undersensitivity and cosine "shoulder" at lower Reynolds numbers. Error analysis shows these current sensors are adequate for many kinematic measurements but may lead to excessive errors when using velocity to calculate dynamical quantities (such as bottom friction, Reynolds stress, or log-layer friction velocities). A careful error analysis must precede any use of these meters for estimating dynamical quantities. These studies pointed out a potential difficulty in using these meters in areas of large ambient turbulence levels (20% turbulent intensities), which are characteristic of many near-bottom shallow water environments. Further study is needed to clarify this behavior.

INTRODUCTION

Field investigations of hydrodynamics and sediment transport in the nearshore zone rely heavily on current measurement. Major studies such as the Nearshore Sediment Transport Study (NSTS) [*Seymour*, 1983] all rely to some degree on estimation of sediment transport by applying current meter data to some transport model, or to verify or establish a new transport model. Flow data are also used to field test models of surf zone hydrodynamics, whereby kinematic quantities are used to estimate dynamical terms in the momentum equation. Examples of terms commonly calculated are advective terms ($u\,\partial u/\partial x$), frictional terms ($f|u|u$), and higher-order moments of the velocity ($\langle u^3 \rangle$).

The present study was motivated by an examination of the NSTS experimental data from Santa Barbara, California, held in February 1980, in which the higher-order velocity moments from current meter measurements showed a time variability not obviously related to time scales of change of the forcing conditions (e.g., wave groupiness), and by field studies that have shown a persistent offshore near-bottom flow that is not satisfactorily explained by nearshore circulation theories. Because of the importance of these quasi-steady flows and higher-order velocity moments on sediment transport modeling in the nearshore zone, the present study was designed to evaluate under carefully controlled laboratory conditions the response of electromagnetic current meters (EMCM) typically used in the field for nearshore sediment transport and combined wave and current flows.

Paper number 5C0360.
0148-0227/85/005C-0360$05.00

All current meters calibrated were electromagnetic, relying on Faraday's law to obtain relative velocity information through use of a fluctuating magnetic field. All instruments were two-axis, with either a 0.040 m (1.6 in.) or 0.105 m (4 in.) diameter sphere, made by Marsh-McBirney, Inc., of Maryland. These instruments were chosen because they are frequently encountered surf zone measurement tools. All calibrations were performed by towing or oscillating the current sensor through the water column.

Previous literature discussing application of Faraday's law to measurement of fluid goes back more than a century. Since that time, a remarkable literature exists on this subject, recently reviewed by *Aubrey et al.* [1984]. Many papers address the theory of electromagnetic flow measurement [e.g., *Shercliff*, 1962; *Bevir*, 1970]. Other studies address the behavior of these current meters from an empirical point of view, most of which is published in unreviewed literature, including extensive tests run by the NOAA National Oceanographic Instrumentation Center (e.g., *Appell* [1977] and much unpublished material). *Cushing* [1976, and earlier work] discussed theory and observations of the behavior of electromagnetic current meters. Most of these studies discussed the steady flow response of electromagnetic current meters, and their vertical and horizontal cosine response. Some limited unsteady testing of these current meters was performed [*Appell*, 1977; *Cunningham et al.*, 1979], which showed that unsteady superimposed motions affected the steady response of these instruments, particularly when the unsteady component was large compared to the steady component. *McCullough*'s [1978] summary graphs of gain versus steady/oscillatory ratio show this dependence well, when the unsteady flow has considerable vertical component. These studies all showed that electromagnetic current meter

response fluctuates measurably as a function of the flow regime. None of the above studies systematically examined the dynamic response of these meters to steady/oscillatory flow, which is a major aspect of the study reported here. The study reported here is described in much more detail by *Aubrey et al.* [1984].

Flow Past a Sphere

Because the electrodes of the electromagnetic current meters discussed here extend into the flow field from the surface of a sphere (see Figure 1), the flow meter is sensitive to the effects of the sphere on the flow field. A brief, qualitative review of flow past spheres is presented below to illustrate the complexity of the flow field and to indicate the resulting difficulty in designing a spherical sensor that has uniform response for all flow regimes. General reference is made to *Schlichting* [1968]; see also *Roshko* [1961] and *Achenbach* [1974].

At low Reynolds numbers the flow around a sphere is laminar, and it is attached to the sphere around the entire perimeter. At Reynolds numbers greater than about 10, the flow is still laminar, but it separates from the sphere at an angle of 80°, measured along the axis of flow from the upstream stagnation point. Between Reynolds numbers of approximately 70 and 5000, a regular von Karman vortex street is present, with periodic vortices shedding from the sphere. Within this range the width of the wake decreases from a value greater than the sphere diameter to a value less than the sphere diameter. For Reynolds numbers between 5000 and 3×10^5 the wake is fully turbulent.

When the Reynolds number (Re) exceeds 3×10^5, the boundary layer on the surface of the sphere becomes partly turbulent. Laminar separation begins but results in turbulent reattachment rather than complete separation, followed by a delayed final turbulent separation. The separation point moves toward the rear of the sphere, ultimately to an angle of about 120°. This causes the familiar dramatic decrease in drag coefficient (drag crisis) observed in laboratory experiments. As the Reynolds number increases, the transition point between laminar and turbulent flow in the boundary layer on the surface of the sphere moves closer to the upstream stagnation point. In addition, the wake width increases as the Reynolds number increases, although it is never as large as the sphere diameter. Finally, at extremely high Reynolds numbers the transition to a turbulent boundary layer occurs sufficiently close to the stagnation point that the flow is largely independent of the Reynolds number.

The above results are modified considerably by roughness elements and unsteady flow. Electromagnetic current meters generally have hydrodynamically smooth insulating exteriors, which are interrupted by protruding electrodes (Figure 1) and mounting stings extending from both the top and bottom of the sensor. Besides the individual wakes generated by each of these protrusions, these three-dimensional roughness elements affect the position of separation on the sphere. Because of their distribution about the sphere, their influence on flow behavior depends on the angle of incidence of the incident flow, as reflected by the cosine response of the instrument [see, for example, *Cushing*, 1976]. Unsteady flow affects the development of flow around a sphere, since the boundary layer will develop with time. Theory and observations provide some guideline for flow development intervals for smooth plates, but these are difficult to apply to spheres with three-dimensional roughness elements.

Also affecting boundary layer behavior are intensities and scales of free-stream turbulence. A number of investigators

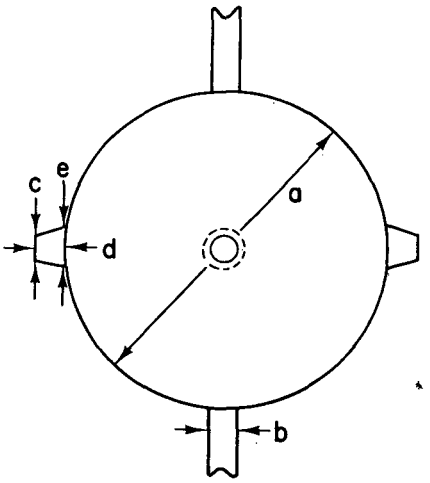

	551M 512/0EM	551
a	4.05cm	10.53cm
b	0.96cm	2.54cm
c	0.50cm	1.15cm
d	0.43cm	1.13cm
e	0.68cm	1.75cm

Fig. 1. Schematic of the large-diameter and small-diameter Marsh-McBirney electromagnetic current sensors, showing primary dimensions and location of roughness elements.

[*Fernholz*, 1978; *Nakamura and Tomonari*, 1982] have shown at values of turbulent intensities (defined as the ratio of the root-mean-square turbulent fluctuations to free-stream velocity) of a few percent, boundary layer thickness and skin friction increase notably, when the scale of the turbulence is comparable to the thickness of the boundary layer. Effects of turbulence at much smaller or larger scales are not well known. As free-stream turbulence intensity increases, the critical Reynolds number for transition to turbulent flow decreases.

Turbulence intensities in the natural environment vary widely. Most reported values are for mid-water measurements, where turbulent intensity (I) is less than 0.1%. *Heathershaw* [1976] measured turbulent intensities of up to 18% in the Irish Sea at 1 m off the bottom. W. D. Grant (personal communication, 1984) typically finds turbulent intensities of 10% or more in water depths of 20–40 m on the continental shelf. *Gross and Nowell* [1983] present data indicating turbulent intensities of 20% at a distance of 70 cm from the bottom in a tidal flow in Puget Sound. In the surf zone, shear-generated turbulence combines with turbulence associated with breaking waves, increasing turbulent intensities over much of the surf zone. No accurate measurements of surf-zone turbulent intensities are available in the literature, however.

The effects of ambient turbulence on boundary layer structure may have profound implications for the use of electromagnetic sensors. Free-stream turbulence is ubiquitous in nearshore environments. In addition, scales and intensities of such turbulence vary greatly, as a function of position from the breaker zone, and as a function of distance above the bottom. If boundary layer growth and separation on the surface of an electromagnetic current meter are sensitive to turbulent scales and intensities, the response of these instruments may change with position in the surf zone and with distance from a boundary. This aspect of current meter sensitivity was

briefly addressed during this study. Some previous experimental work on this subject was performed by *Bivins* [1975] and *Griffiths* [1979].

In summary, flow structure around spheres is complex and varies with the nature of the incident flow and geometry of the sphere exterior. This complexity suggests that EMCM response to nearshore wave and current conditions may be variable. The present study investigates this possibility empirically.

CALIBRATION METHODOLOGY

Current Meters and Calibration Facilities

Sixteen current measuring instruments were calibrated as part of this study, representing five different types of current meters. These instruments include four Marsh-McBirney MM551 current meters, seven Marsh-McBirney MM551M current meters, three Marsh-McBirney MM512/OEM current meters, and Sea Data 635-12F and 635-9 directional wave gages. Calibrations were carried out at the flume-tow tank facility at the Woods Hole Oceanographic Institution (WHOI) and the ship model test basin at the Ralph Parsons Laboratory at the Massachusetts Institute of Technology (MIT).

The Marsh-McBirney MM551 consists of a 10.5-cm-diameter electromagnetic sensing sphere (Figure 1) which is rigidly connected to a stainless steel pressure case. Because of the sensitivity of these instruments to electromagnetic noise, they were all calibrated at the MIT facility, which has a lower noise level than the WHOI facility. The Marsh-McBirney MM551M is a modified version of the MM551, with a 4.0-cm-diameter sensing sphere (Figure 1) connected to the electronics case by cable. Six of the MM551M were calibrated at the WHOI flume facility, while two (including one also calibrated at WHOI) were calibrated at the MIT facility. The Marsh-McBirney MM512/OEM is physically similar to the MM551M. The MM512/OEM were all calibrated at the MIT facility.

Finally, Sea Data 635-12F and 635-9 directional wave gages use an electromagnetic flow sensor (Marsh-McBirney MM551 and MM512/OEM, respectively). The Sea Data 635-9 is described in more detail by *Aubrey and Hill* [1984], and its behavior in a field intercomparison described by *Grosskopf et al.* [1983]. The 635-9 was calibrated at the WHOI facility, while the 635-12F was calibrated at the MIT facility.

The WHOI flume and tow tank facility is 1.2 m wide, 21.3 m long, and 1.67 m high. The tow cart is a self-propelled platform riding on two aluminum rails attached to the top of the tank side walls. Motion is achieved by frictional contact of two rubber drive wheels with the aluminum rails, and propulsion is provided by a variable speed electrical motor and analog reducing transmission. Cart speed is determined from elapsed time electronically measured between two points along the tank. The tow cart has a speed range of 0–1.18 m/s over a test section of 9 m. Calibrations were run with water depths between 1.25 and 1.5 m. The flow sensor was attached to the cart via a mounting device that allowed angular rotation about the vertical axis.

The MIT facility is a ship model test tank, operated by the Ocean Engineering Department of MIT. The tank is 2.61 m wide, 32.93 m long, with a normal water depth of 1.22 m. The test section length is 16.0 m, with a pair of optical sensors at either end of the test length determining elapsed time. The tow cart is a platform suspended above the tank on two metal cylinders running the length of the tank. Propulsion is by a tensional steel band connected to an electric motor through three gear boxes in series. Speed varies by changing the gear ratio in one or more of the gear boxes. The maximum speed used in the tow tank was 2 m/s.

Oscillatory flow calibration is performed at this MIT tow tank facility using an in-line device (Figure 2) capable of rotation in the horizontal plane to any desired angle with respect to the mean flow. The maximum peak-to-peak amplitude of the horizontal oscillatory motion is 0.5 m, with a variable period from about 1 to 12 s. Period control for the oscillator allows a continuum of periods through use of a variable speed motor, but amplitude control is through a cam arrangement that allows 25 distinct peak-to-peak amplitudes of oscillation.

Statistical Methods

Statistical techniques applied to analyze calibration results are discussed in detail by *Aubrey et el.* [1984]. Emphasis is placed on linear models with one or more independent variables (x), where voltage is the dependent variable (y). Independent variables are generally dynamical terms from the equations of motion (see next section). The basic model is

$$y = \alpha + \sum_{i=1}^{m} \beta_i x_i + \varepsilon \tag{1}$$

where m is the number of independent variables, α and β_i are coefficients, and ε is an error with zero mean and variance σ^2. Estimates of α and β are represented as $\hat{\alpha}$ and $\hat{\beta}$. β represents the sensitivity (units: V m s^{-1}) of the instrument, in our usage, as distinguished from the gain, which is the inverse of the sensitivity. Since our interest is the response of current meters, most results are in terms of sensitivity. The offset consists of two parts. Electronic offset is the measured voltage derived from an immersed sensor with no water flowing past it. Numerical offset refers to the value of $\hat{\alpha}$ calculated from the data removing the electronic offset. For a purely linear instrument, numerical offset would be zero. The $\hat{\alpha}$ and $\hat{\beta}$ and their variances are determined using standard least squares procedures, which also provide estimates of the error ε. The F-test [*Draper and Smith*, 1966] is used to determine level of significance of the least squares fit using the error variance (from which the correlation coefficient is derived). Alternatively, error bounds on the sensitivity, $\hat{\beta}$, can be derived using the t-test, as can the error bounds for the offset, $\hat{\alpha}$.

Dimensional Analysis

Dimensional analysis provides a convenient tool for designing a calibration strategy in pure steady, pure oscillatory, and combined steady and oscillatory flows. For steady flow, we select as dimensional parameters the free-stream velocity (U), the kinematic viscosity (ν), and the diameter of the current meter probe (d). According to the Buckingham-π theorem, one-dimensionless grouping derived from these three variables determines the flow field. For example, we can write

$$U = \bar{U} f(Ud/\nu) \tag{2}$$

where UD/ν is the steady Reynolds number (Re_s) and $\bar{U}$ is an average velocity sensed by the current meter.

For pure oscillatory flow, there are four characteristic parameters: peak-to-peak amplitude of oscillation (A), period of oscillation (T), dimension of current meter (d), and kinematic viscosity (ν). Any two of the following three dimensionless groupings can be chosen to represent a functional depen-

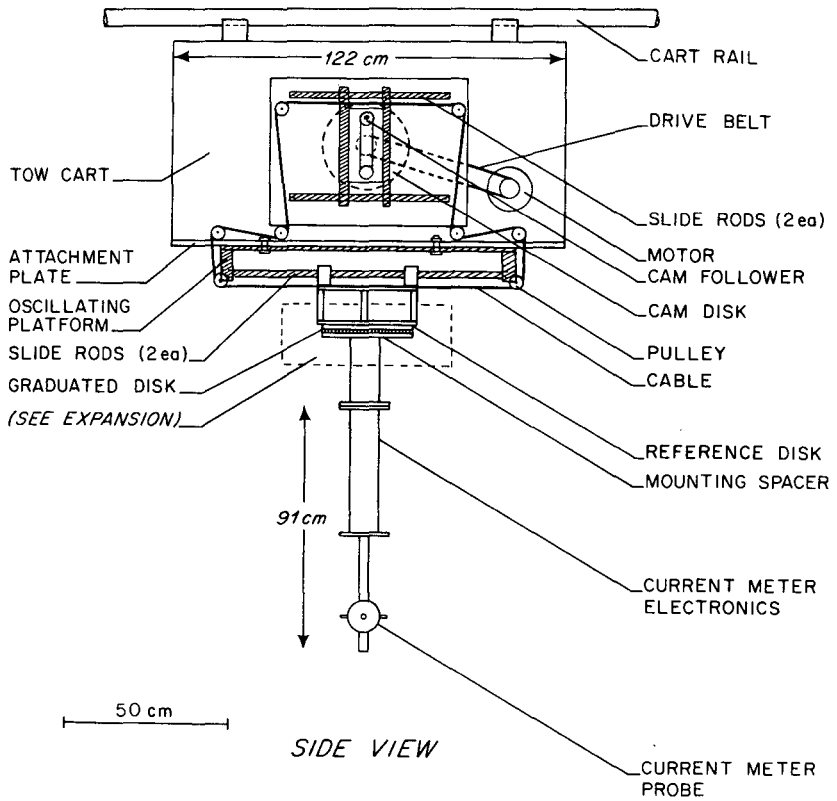

OSCILLATING MECHANISM FOR M.I.T. TOW CART

Fig. 2. Slosher for generating horizontal oscillatory flows in the MIT ship model test facility. An MM551 current meter with attached housing is mounted on the slosher.

dence: A/d, $(Ad)/(vT)$, vT/d^2. We could choose, for instance,

$$\bar{U} = \frac{A}{T} f\left(\frac{A}{d}, vT/d^2\right) \tag{3}$$

Each of these dimensionless groupings has a physical significance. The quantity A/d is readily shown by a straightforward order-of-magnitude analysis to be the ratio of the unsteady to convective terms (linear versus nonlinear inertial terms) in the governing equations. It can be shown by a simplified theoretical analysis [e.g., *Mei*, 1983] that the parameter A/d controls flow separation. Experiments on circular cylinders indicate that flow separation occurs if $A/d > \sim 1$. The parameter A/d is sometimes termed the Keulegan-Carpenter number. The quantity $(Ad)/(vT)$ is analogous to the terms Ud/v in steady flow, and can be considered as an oscillatory Reynolds number (Re_0). A straightforward order-of-magnitude analysis indicates that $(Ad)/(vT)$ represents the ratio of nonlinear inertia terms to viscous terms in the governing equations. If Ud/v is important for steady flows, then $(Ad)/(vT)$ is expected to be important in unsteady flows, especially if $A/d \gg 1$. The parameter vT/d^2 can be interpreted as the ratio of the squares of the linear, oscillatory laminar boundary layer thickness to current meter dimension. This interpretation is relevant only for small A/d.

For combined steady and oscillatory flows, we choose the following six characteristic parameters to represent the flow field: free-stream velocity (U), peak-to-peak amplitude of oscillation (A), period of oscillation (T), current meter dimension (d), kinematic viscosity (v), and angle between steady and oscillatory flow (ϕ). As in the previous cases of pure steady and pure oscillatory flows, we assume zero vertical component to these flows, since our tests were for purely horizontal flows. In near-surface applications where vertical oscillatory motions are appreciable, this dependence must be included. From the six characteristic parameters, four dimensionless groups can be determined which specify the flow completely. We list six possible dimensionless groups whose importance we can test experimentally: UT/A, UT/d, vT/d^2, Ad/Tv, Ud/v, A/d, and ϕ. All groupings have been discussed previously except for UT/d and UT/A. The quantity UT/d can be interpreted as the inverse of a Strouhal number, and UT/A is proportional to the ratio of the steady velocity to the maximum orbital velocity. *McCullough* [1978] and others use the latter dimensionless quantity in their discussions of sensor performance in combined steady and oscillatory flow.

RESULTS

Experiments on EMCM response were divided into five primary categories. Specific questions addressed in each category depend on characteristics of flow past a sphere which were described earlier. An outline of the five major categories with the principal scientific problems addressed under each category is presented below. Detailed presentation of these results can be found by *Aubrey et al.* [1984].

Pure Steady Flow

Twenty-one current meter calibrations performed on 16 instruments under steady flow conditions (Figures 3 and 4) form the basis for interpretation of steady flow behavior. Six of these calibrations were for Marsh-McBirney MM551 10.5-cm-

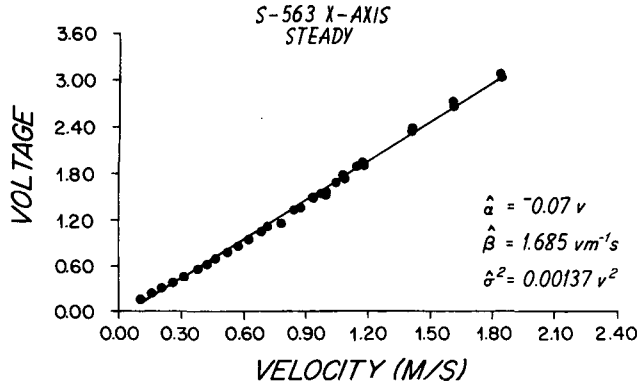

Fig. 3. Output voltage versus tow velocity for x axis of S563 for pure steady conditions. As in the following figures, regression estimates of fit are indicated on the figure; specific information can also be obtained from tables in *Aubrey et al.* [1984].

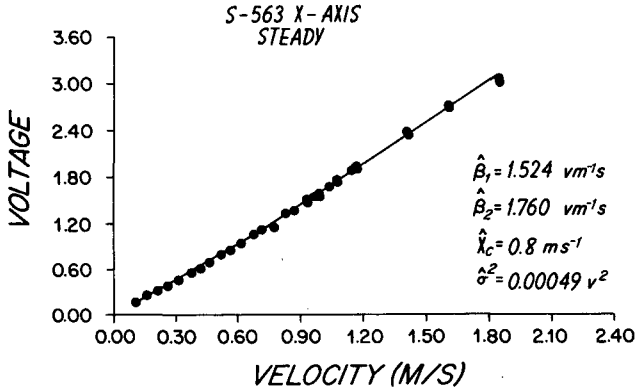

Fig. 4. Two-segment results for the same two tests of the previous figures, with a critical velocity of 0.8 m/s (representing the smallest error variance of any critical velocity).

diameter spheres; the remainder were for MM512/OEM 4.0-cm-diameter spheres. Number of data points per calibration and speed increment varied slightly as a function of calibration facility. In most cases, both axes were calibrated. In summary form, the results for steady flow are:

1. Nonlinear meter response results in an rms deviation of 0.042 V in numerical offset, α, between the manufacturer specification and observed values (corresponding to approximately 2.5 cm/s in velocity). This offset reflects the nonlinear dependence of sensitivity on flow speed. The electronic offset was removed during data analysis.

2. Observed sensitivites of the current meters differed from manufacturer's specifications by an average of 5.3% (0.086 V/m/s root-mean-square sensitivity). Maximum deviation was 11%, observed on four sensors. Many of these instruments had not undergone field deployment before calibration. The sensitivity incorporates the quantity (d/v) from the Reynolds number, so the model tested was

$$\text{voltage} = \beta \text{ velocity} + \alpha + \varepsilon \tag{4}$$

In all normal runs, the single regression fit is significant at the 95% level.

3. Calibrations following deployments can differ significantly from those preceding deployment if biological growth is significant. Changes in sensitivity of 25% can result from biological fouling, but magnitude of gain changes depends on type of fouling.

4. Sensitivity imbalances between two axes of the same current meter were 4.8% of the expected sensitivity (root-mean-square difference).

5. A two-segment least-squares fit (Figure 4) to the data consistently resulted in lower error variance compared with the single segment least squares fit. The velocity cutoff separating the two line segments is determined in a least squares fashion, testing the hypothesis that sensitivity changes with Reynolds number due to transition from laminar to turbulent flow. In spite of the improved fit with the two-segment model, there was no consistency in cutoff Reynold's number among all the current meters to suggest that this improvement in gain is due to dynamical causes. Large spheres had a mean cutoff value of $Re = 1 \times 10^5$, while smaller spheres had a mean cutoff at $Re = 3.1 \times 10^4$, an order of magnitude below that at which "drag crisis" occurs for a smooth sphere in well-behaved flow. A higher-order polynomial fit or a multisegment least squares fit will reduce error variance compared to a linear regression, but data do not support any dynamical interpretation for the position of a velocity cutoff in a two-line segment model.

Pure Oscillatory Flow

Four sensors were calibrated in pure oscillatory flow, with periods ranging from 1 to 12 s, and double amplitude ranging up to 0.5 m. Results are based on peak-to-peak velocities (both positive and negative), to eliminate electronic offset. Complete details of analysis procedures are contained in *Aubrey et al.* [1984]. These test show:

1. Sensitivity is approximately the same (within 2%; Figure 5) in oscillatory flow as in pure steady flow.

2. Because of nonlinearity in sensitivity, offsets are significant for oscillatory flows. If these offsets are not removed, apparent oscillatory sensitivity will be erroneously high.

3. Unsteady results show a sensitivity dependence on A/d and $(Ad)/(vT)$, which has no obvious physical explanation.

Combined Steady/Oscillatory Flow

To simulate surf zone and inner shelf hydrodynamics in the laboratory environment, tests were conducted with combined steady and oscillatory motions. Steady motions were simulated using the tow cart at the MIT facility, while oscillatory motions were created with a specially constructed slosher (Figure 2). Oscillatory motion was rectilinear in a horizontal

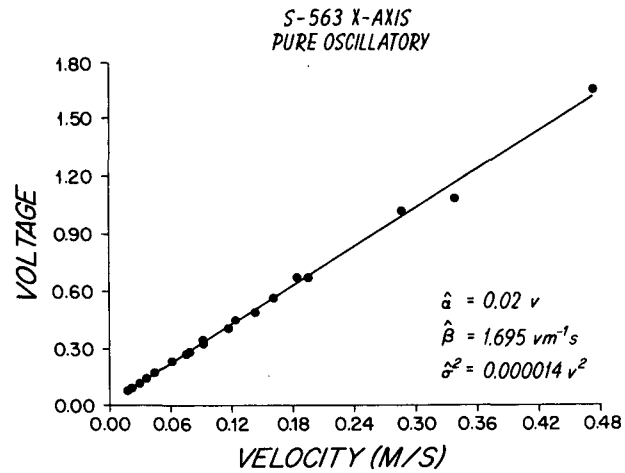

Fig. 5. Output voltage versus peak orbital velocity for pure oscillatory flow.

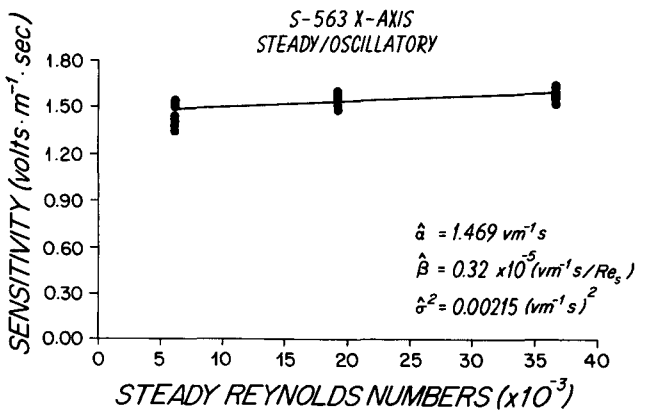

Fig. 6. Steady sensitivity as a function of steady Reynold's number for combined steady/oscillatory flow conditions. Sensitivity increases with *Re*.

plane to simulate shallow water orbital motions. Most tests were conducted with colinear steady and oscillatory motions; some were conducted with oscillatory motions at right angles to the steady motion. Two current meters underwent this extensive steady/oscillatory testing: a Marsh-McBirney MM551 sensor with a 10.5-cm-diameter sphere (B501), and a Marsh-McBirney MM512/OEM sensor with a 4.0-cm-diameter sphere (S563). Results are divided into two sections: the effect of combined steady/oscillatory flow on steady flow sensitivity, and the effect of combined steady/oscillatory flow on oscillatory sensitivity.

Major results of the tests of steady flow sensitivity are:

1. Steady sensitivity for sensor S563 (Figure 6) is 10% lower in combined steady/oscillatory flows than for pure steady flows. This sensitivity is significantly related to A/d and Ud/v (at the 95% confidence level), but has no relation to UT/A or UT/d. For sensor B501, mean steady sensitivity was lower by 7.1% for combined steady/oscillatory tests as compared to pure steady tests. Sensitivity is significantly related to Ud/v and UT/d, but not A/d, $(Ad)/(vT)$, or UT/A (at the 95% confidence level).

2. Decrease in steady sensitivity is qualitatively consistent with the complex wake structure set up in the combined tests versus pure steady tests.

3. Error variance for regression model fits was increased by a factor of 1.5–3 for sensor S563, but increased 5–7 times for sensor B501. The larger sphere was more severely affected by oscillatory motion than the smaller sphere.

The results of the test of oscillatory flow sensitivity are:

1. Oscillatory sensitivity in combined steady/oscillatory flow is consistently less than oscillatory sensitivities for pure oscillatory flows. For S563 (Figure 7), this decrease in sensitivity is 8.5%, while for B501 the decrease is 14.5%. These differences are significant at the 95% confidence level.

2. Oscillatory gain for S563 is significantly correlated with all nondimensional groupings (Ud/v, A/D, UT/d, and $(Ad)/(vT)$) with the exception of UT/A. This lack of correlation with UT/A is surprising because it is the ratio of steady to oscillatory velocities, which has been used by other investigators [e.g., *McCullough*, 1978] to discuss sensor dependence on unsteady flows. For B501, oscillatory sensitivity is significantly correlated with Ud/v, UT/d, and $(Ad)/(vT)$, but not with UT/A or A/d. Again, lack of dependence on UT/A (which ranged from zero to 30 in the calibration runs) is surprising in light of previous observations by other investigators.

Horizontal Cosine Response

Two sensors were calibrated for horizontal cosine response, a large sphere (B498) and a small sphere (S563, Figure 8). Calibrations were performed at 5° (S563) or 10° (B498) increments from 0° to 360°, with each degree increment towed at three different steady speeds. The experimental set-up enabled us to accurately measure relative angle changes, with accuracies of a fraction of a degree using machined spacers. Absolute direction referenced to the axis of the MIT tow carriage was difficult to establish to better than 2°–3°. To circumvent this problem, we minimized the mean-square-error of the measured cosine response to predicted cosine response, as a function of angle, yielding an improved estimate of the absolute orientation of the current meter with respect to the tow cart axis. The results of this study are:

1. Average sensitivity (over all angles) for each of the axes and at each of three Reynolds numbers is dependent on Reynolds number, with sensitivity increasing with Reynolds number. Sensitivities are consistently lower than comparable sensitivities for on-axis steady tow results. This lowered sensitivity is consistent with an intercardinal undersensitivity in horizontal cosine response, with greatest undersensitivity at low Reynolds number. Detailed examination of horizontal cosine response demonstrates this intercardinal undersensitivity, and its trend with Reynolds number.

2. Because of the nonlinear sensitivity observed in these meters, response to off-axis flows near 90° shows large errors in normalized sensitivity.

3. There is a shoulderlike structure in the cardinal sensitivity, particularly for lower Reynolds number. Near 0° relative flow, normalized sensitivity is low. The sensitivity rises as the relative angle increases to about 20°, finally turning to undersensitivity as the angle increases further. This near-cardinal behavior is likely due to asymmetries in sensor geometry as the protruding electrode is slowly rotated away from the forward stagnation point.

4. Root-mean-square error in horizontal cosine response (minimized according to the procedure outlined earlier in this section) varies as a function of axis and Reynolds number. Errors increase with Reynolds number for both axes. These errors are comparable in magnitude to those arising from steady tow results. Residual errors plotted as a function of tow angle relative to the stagnation point are larger as the sensor is rotated away from head-on tow directions, for all Reynolds numbers. This may be a partial reflection of the numerical offset resulting from nonlinear gains.

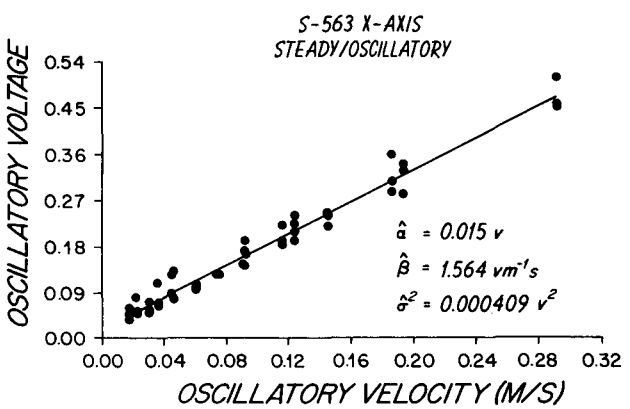

Fig. 7. Oscillatory voltage versus peak oscillatory velocity under combined steady/oscillatory flow conditions. Although the regression is excellent, the sensitivity is lower than in the pure oscillatory case.

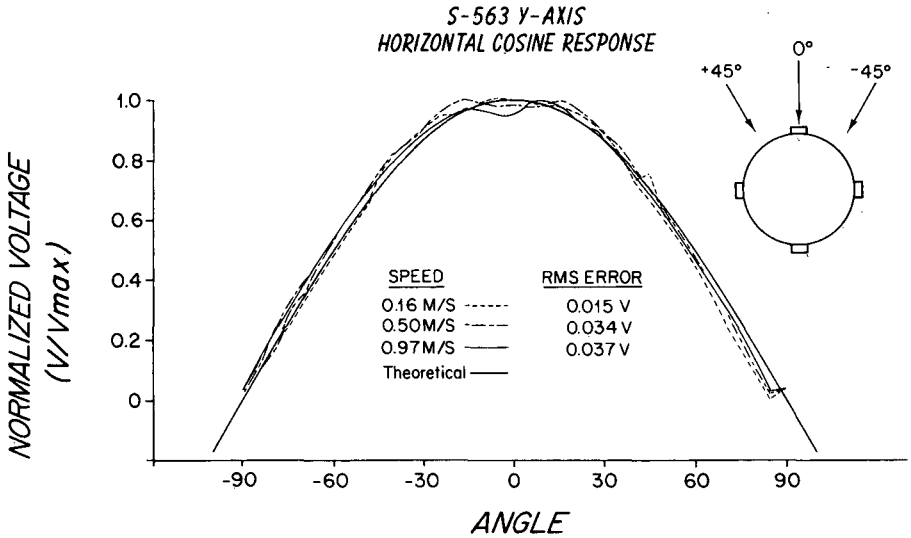

Fig. 8. Horizontal angular response for S563, *y* axis, at three different tow speeds. Note "shoulder" about the 0° flow direction indicative of asymmetry of roughness distribution on sphere at low angle of attack.

5. For B498, the mean sensitivity varied as a function of Reynolds number, although not in as predictable a manner as the smaller sphere. Up to a Reynolds number of 53,000, the mean sensitivity increased, but decreased slightly at a Reynolds number of 101,500. Mean sensitivities for all horizontal cosine tests were less than sensitivities for on-axis steady flow tests, demonstrating the intercardinal undersensitivity observed in the other sensor. Greatest undersensitivity occurs at low Reynolds number. Detailed examination of individual combinations illustrates this undersensitivity [*Aubrey et al.*, 1984].

6. For low Reynolds number, there is also evidence of the cosine "shoulder," responding to a sensitivity to electrode position near the forward stagnation point.

7. Root-mean-square errors steadily increase as Reynolds number increases, ranging from a low error of 0.011 V to a high of 0.046 V, or 0.01 m/s up to 0.31 m/s in velocity. Residuals are largest for off-axis flows, least for nearly head-on conditions. These results are consistent with those determined from the smaller sensor, S563.

Grid Turbulence Results

As a small part of this study, we investigated the effect of free-stream turbulence on sensor response using two grids towed in front of the current sensor S563, at varying tow speeds (Figure 9). Briefly, tests showed the following:

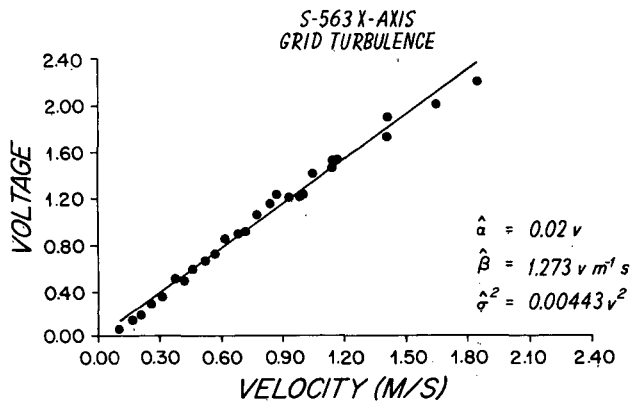

Fig. 9. Output voltage versus tow velocity behind grid 2 turbulence. Scatter is relatively low, while sensitivity is much decreased compared to pure steady conditions. This decrease cannot readily be explained by flow blockage.

1. Sensitivity of current meters decreased by 24% and 45% for the two grids for the grid-turbulence runs compared to the quiescent steady tow results.

2. A simple model of blockage behind grids [*Aubrey et al.*, 1984] shows that grid 1 results can be explained by flow blockage, even though experimental results where blockage was obvious were not used in the analysis. However, grid 2 results cannot be explained by blockage, indicating that either the sensor was not working or that increased intensity of turbulence behind grid 2 caused a hydrodynamic effect registered as a large change in sensitivity.

3. Error variance for grid 1 tests were significantly higher than seen during pure steady tests in calm water, but error variance for grid 2 was lower compared to pure steady tests in calm water. This indicated that the sensitivity change may be due to hydrodynamic effects.

4. Grid turbulence results reported here are preliminary because the methodology did not adequately separate sensor effects and tow cart behavior. While future studies are necessary to elucidate this behavior, the present study does suggest that care should be taken when inferring dynamical quantities from measurements made with electromagnetic current meters in highly turbulent flows. We hope to clarify this behavior in the future.

DISCUSSION AND CONCLUSIONS

Experimental results on the dynamic response of electromagnetic current meters demonstrate a complex behavior in steady and oscillatory flows which must be considered in interpretation of these data. Results show EMCM sensors to be useful for a variety of environmental applications; however, for other more rigorous applications, these sensors may not be suitable. To determine the sensor's utility for any application, a careful error analysis is required, using the present or analogous results to estimate statistical variability.

Because flow structure around a sphere is complicated, one would expect spherical EMCM's to have limitations. Not only is the boundary layer structure a function of flow *Re*, but wake structure around blunt bodies is also complex. Add to this large roughness elements, nonuniformly distributed about

the sphere, and the wake structure becomes even more complicated. Results show sensitivity of these sensors to be nonlinear, demonstrated by the presence of a numerical offset (distinguished from an electronic offset) and the better two-segment linear-fit model as compared to the single segment best fit model. The cutoff in the two-segment model was not linked to any boundary layer phenomenon, such as transition point between laminar and turbulent flow. This is partly attributed to the influence of protruding electrodes and mounting gear, which cause a transition at a lower Re (3×10^4 to 1×10^5) than predicted from experiments on smooth spheres ($Re = 3 \times 10^5$). The scatter in these transition values and significant difference in critical Re for large versus small spheres, however, argue against the interpretation of x_c as the transition Reynolds number. In fact, x_c may be solely a statistical result, not a dynamical one. The better fit obtained using multisegment or polynomial models is useful for calibration and analysis purposes, even if it is not linked to any clearly defined dynamical effect.

Although single-segment linear models relating voltage output to tow speed show significant fits, mean errors are on the order of 1–5 cm/s. Differences in sensitivity of 10% between axes and departures from manufacturer calibrations emphasize the necessity of careful, frequent calibrations for sensitive experiments.

The nonuniform distribution of roughness elements and complicated flow structure leads to an Re-dependent horizontal cosine response. Undersensitivity as high as 25% leads to rms errors in velocity (for a particular Re) of 1–3 cm/s. Largest residues or errors occur when flow is 90° away from head-on. This characteristic is due largely to wake structure and position of electrodes within or outside the wake. Furthermore, response is sensitive to small changes in flow direction near the cardinal axis, as an electrode rotates from its position at the forward stagnation point. This Re-dependent behavior gives rise to a calibration "shoulder" in the horizontal cosine response.

Steady flow sensitivity may also be affected by free-stream turbulence intensity and scales. Although experiments in this study are not conclusive, they suggest differences in steady sensitivity when free-stream turbulence intensities exceed about 1%, and energetic turbulent scales are the order of the roughness (electrode) size. Implications of this result for inner shelf and surf zone measurements are profound, since turbulence scales and intensities vary widely over short separations. This possibility reinforces the need for careful, controlled follow-up studies to examine this behavior in detail. Previous studies of this effect [*Bivins*, 1975; *Griffiths*, 1979] have suffered from nonhomogeneous turbulent field and limited range of turbulence scales and intensities. If sensor performance is as dependent on turbulent properties as suggested here, then the spherical EMCM's have limited utility in surf zone studies (where turbulence intensities commonly exceed 20%) unless the sensor dependence on turbulent properties can be predicted empirically or theoretically.

Steady flow around a sphere is distorted by roughness elements, whether they be electrodes, mounting brackets, or biological growth. In addition, the untreated metallic surfaces on the EMCM sensor head (the mounting brackets and electrode faces) are prone to biological growth. Tests show a 26% decrease in sensitivity following a 2-month deployment. Once the sensor was lightly scrubbed to remove biological growth, sensitivity returned to its predeployment level. Since sensitivity was more altered at large Re than small Re, most of the fouling effect was hydrodynamic.

Flow around spheres becomes more complex when oscillatory motions are introduced, especially when orbital amplitudes are only slightly larger than, or smaller than, the sphere diameter. As flow reverses, the boundary layer must redevelop, the wake structure must stabilize, and pressure gradients readjust. Time scales for these processes can be of the order of the orbital period, causing a chaotic, unsteady flow structure. For particular periods, forces are exerted on the sphere that can cause sphere movement if the sphere is not rigidly attached.

Our experiments showed no significant differences between pure oscillatory and pure steady sensitivity. Oscillatory sensitivity is significantly correlated with A/d and $(Re)_0$, but not Tv/d^2, suggesting laminar boundary layer thickness is not important in EM sensor behavior. Sensitivity generally decreases with increasing A/d and increasing $(Re)_0$, which behavior has no obvious physical explanation. Finally, oscillatory behavior showed the importance of including the numerical offset in sensitivity calculations, since neglect of this offset resulted in an average 8% change in apparent oscillatory sensitivity (increased sensitivity, since offsets were not positive).

Flow structure around spheres is increasingly complicated under combined steady and oscillatory flows. Intuitively one can see the effect if $u_m > U$, since flow would actually reverse over an oscillation, similar to pure oscillatory conditions. However, even for $u_m < U$, unsteady effects will alter significantly the measurement of steady flow components, changing local pressure distributions around the sphere. Since inner shelf and surf zone environments are generally characterized by combined wave/current flows, our tests were particularly relevant.

Steady flow was combined with horizontal oscillatory flow, both for colinear and perpendicular conditions. Under these combined conditions, steady sensitivity decreased by 7–10%, with a dependence on the nondimensional grouping of $(Re)_s$, but not consistently with A/d, $(Re)_0$, UT/d, or UT/A. Sensitivity increases with $(Re)_s$. Error variance increases in these combined flows as well, increasing by up to 70%, and sometimes more.

As with the steady case, oscillatory sensitivity decreased under combined flow conditions over the range of 9–21%. This decrease in sensitivity is consistent with the notion of complicated wake behavior. Oscillatory sensitivity is significantly correlated with $(Re)_s$, UT/d, and $(Re)_0$, with less correlation with A/d and none with UT/A. Lack of dependence on UT/A was not expected.

Combined steady/oscillatory flows are shown to alter response of spherical EMCM's, attributable in large part to changes in wake structure under this complex flow situation. Although induced currents, or streaming, were not directly observed in this study, changes in numerical offsets and variable sensitivities combine to produce an apparent steady flow. Numerical offsets of up to 4 cm/s were calculated, which would result in an apparent steady flow if not properly accounted for. These apparent flows never exceeded 10 cm/s.

The complicated response of EMCM's to varying hydrodynamical conditions makes analysis of EMCM data difficult. Several options are available. The most commonly used option is to ignore these dynamical effects and apply either the manufacturer's calibrations or steady flow calibrations. This study clearly shows that such an option is short sighted unless an error analysis indicates that the required accuracies are much less than the errors in response. The second option is to use results from this study to calculate errors associated with any particular use of the data, and judge if those errors are acceptable. If accuracy is still sufficient for a given use, then

the data can be used for that application with appropriate errors. If accuracy is not good enough, then either a more precise calibration is required (such as a multisegment or polynomial model fit or even a more complete dynamical gain description), or another instrument must be selected. A third option is to provide a complete dynamical description of current meter response to ambient flows, and correct the data according to this response. This approach requires either a complete understanding of dynamical behavior of spherical sensors, or extensive and exhaustive testing of each current meter used. *Smith* [1978] provides an iterative procedure for correcting for angular response. *Aubrey et al.* [1984] describe an iterative procedure to account for dynamical sensitivity dependence.

Similar corrections can be made for a known frequency response, using the transfer function. Generally users of EMCM's specify a time constant for a particular application, depending on the frequency band of interest. These time constants arise from analog electrical filter characteristics of the particular instrument. It is erroneously assumed that the frequency response for an instrument guarantees a constant transfer function, $L(f)$, and an ability to resolve scales that are contributing to high-frequency components. In fact, spatial averaging prevents resolution of many of these higher-frequency components, in a manner often approximated using Taylor's frozen turbulence hypothesis. Given the averaging volume of an EM sensor (approximately 2–3 sphere diameters in scale), one can compute the frequency cut-off for energetic turbulent flows in any steady current U. Second, the filter cut-off is often the -3 dB point of the filter, when the transfer function has decreased to a level of 50% the unfiltered value. This is of little concern if energetic motions are confined to frequencies well below the cut-off frequency, but can lead to aliasing and erroneous spectral estimates when frequency of energetic motions is close to or higher than the cut-off frequency. Corrections for the frequency response can be made easily in the frequency domain, by inverting the transfer function. Corrections can also be done in the time domain by deconvolution, generally an expensive procedure. A safe strategy to avoid these problems is to assure that the cut-off frequency is well above any energetic motions that would be sensed by the current meter.

Simpler processing alternatives exist. For instance, depending on the ratio UT/A (steady Re divided by oscillatory Re), one could assign a gain for the steady component which is of neutral sensitivity (no oscillatory flow) or undersensitive (comparable oscillatory flow). Similarly, for the oscillatory component, a variable gain could be applied depending on this same ratio. Such gain corrections would best be applied as spectral corrections: once the spectrum is calculated, mean flows are corrected for undersensitivity and noncosine response, while oscillatory gains are corrected and distinguished from steady gains. This must proceed on a meter-by-meter, axis-by-axis basis.

To illustrate the impact of these hydrodynamically dependent flow meter responses on various applications of these data, we consider briefly four cases: (1) estimation of velocity for kinematic purposes; (2) use of arrays of EMCM's for log-law estimates of u_*; (3) use of EMCM's for directional wave estimation; and (4) estimation of higher-order velocity moments for sediment transport purposes.

Estimation of Velocity for Kinematic Purposes

For pure steady or pure oscillatory flows, errors are relatively small, with standard deviations of 1–5 cm/s. Errors can be reduced significantly by higher-order fits, using either multiple-segment linear regression or higher-order polynomial regression. Using different gains for each axis, careful calibrations should yield rms errors of less than 1–2 cm/s, for limited Re ranges. Care must be taken to minimize effects of biofouling on degradation of gain. Deviations from cosine response can be easily accounted for in numerical analysis procedures, either in real time or following the experiment. These accuracies, however, all depend on obtaining good electronic zeroes or offsets in the field.

Combined steady/oscillatory flow considerably degrades sensor response, and steady and oscillatory gains commonly may have errors of 10% or so. Errors in combined steady/oscillatory conditions are larger than for pure steady or pure oscillatory flows by a factor of 2 or more. Magnitude of errors also depends on the impact of free-stream turbulence on sensor performance. The present study suggests sensitivity depends on turbulent intensity and scale. Since the present experiments were neither complete nor exhaustive, this effect is only a possible source of degradation in sensor performance, which must be examined more fully.

Use of Arrays of EMCM's for Log-Law Estimates of u_*

For suitably behaved boundary layers, there is a constant stress region whose turbulence level can be calculated a variety of ways: logarithmic-law, eddy correlation, and inertial range dissipation estimates. Examining the logarithmic law only, we need to consider the appropriate statistics for obtaining significant estimates of u_*. The friction velocity, u_*, is obtained from a least squares fit of mean velocities at a number of vertical positions above the bottom. We can use the F-test to establish a null hypothesis limit for our estimates of u_*, by calculating the probability that u_* is different from $2u_*$ or 0 at the 95% confidence level.

For $N = 3$, we need an R^2 value of 0.994 before the null hypothesis is invalidated. For $N = 4$, we need an R^2 of 0.902 before the null hypothesis is invalidated. For the case of $N = 2$, R^2 cannot be tested because there will always be a perfect fit between two points. Tests for 95% confidence limits on any multiple of u_* can be made using the t-test, if var (u_*) is known or calculated.

Numerical experiments for the EM sensors tested here show that 95% confidence fits are possible for pure steady flows with low free-stream turbulence levels if the EMCM's are carefully calibrated. For sensors that are exposed to high-intensity free-stream turbulence or for sensors with significant unsteady, oscillatory components, these criteria may be rarely met. For gain uncertainties of 10% or more, and unstable electrical or numerical offsets, these criteria preclude the use of EMCM's for precise (95% confidence limits) estimates of u_*.

For similar reasons, and adding on other error sources associated with determining an appropriate vertical reference direction, eddy correlation techniques are difficult to apply to field data acquired with EMCM's if strong oscillatory motion is present or possibly if free-stream turbulence levels exceed a low threshold.

Use of EMCM's for Directional Wave Information

Grosskopf et al. [1983] discuss the use of EMCM's for directional wave estimation, when deployed in conjunction with a pressure sensor. The current meter data can be used to determine the frequency spectrum of the sea surface elevation, as well as the directional properties of waves. For use as indicators of sea surface variance, the unsteady gain of the instrument must be well known. Experience by the authors has

shown sea surface variances calculated using pressure data and velocity data agree well (within 10%), suggesting that for these conditions the steady gain applied is close to the true oscillatory gain. Comparison of sea surface variance for pressure and velocity data provides a useful check on current meter performance and extent of fouling.

Because directional estimates rely on ratios of products of pressure and velocity autospectra and crossspectra, gains for each of these functions must be known to at least a common multiple. For instance, separate gains for x and y axis are required to obtain good directional information. If not accounted for, the 5–10% difference in gain between sensor axes observed in this study will degrade directional estimates. Preferably, gains derived from combined steady/oscillatory calibrations should be applied, rather than those from pure steady, although this is difficult and expensive to do routinely. Accurate numerical offsets are also crucial to good directional estimates, as an incorrect numerical offset will bias the estimate.

If free-stream turbulence levels are critical to EMCM calibration, flow sensors should be removed from the more energetic part of the turbulent bottom boundary layer. Directional estimates can be seriously degraded by biofouling, as indicated by the present experiments on a "dirty" probe following a 2-month deployment, compared to that same probe before deployment. Gain degradation was different for the x and y axes, indicating that any directional information derived from such a sensor would be in error after biofouling began.

Estimation of Higher-Order Velocity Moments for Sediment Transport Purposes

A common use of current meter data is estimation of sediment transport rates using a higher-order moment of the velocity signal. For instance, the third moment of velocity, $\langle u^3 \rangle$, commonly is assumed to be proportional to sediment transport rate. If we know the errors in estimating u, we can make estimates of errors in $\langle u^3 \rangle$.

As a simple model, we assume that

$$u = u' + \varepsilon$$

where u is the true velocity, u' is the observed velocity, and ε is the error in the observation. We can then calculate $\langle u^2 \rangle$

$$u^2 = uu = u'^2 + 2u'\varepsilon + \varepsilon^2$$

and then $\langle u^3 \rangle$:

$$u^3 = u'^3 + 3\varepsilon u'^2 + 3\varepsilon^2 u' + \varepsilon^3$$

In this latter case, our relative error is approximately $3\varepsilon(u')^2/(u')^3 \simeq 3\varepsilon/u'$, whereas the relative error in u is ε/u'. Our relative error in $\langle u^3 \rangle$ therefore is 3 times that in u. For a ratio $\varepsilon/u' = 0.1$ (a 10% error in gain), relative error in $\langle u^3 \rangle$ is about 0.33, an unacceptable error in many situations. For an error ratio $\varepsilon/u' = 0.45$ (characteristic of the error observed in a dirty probe calibration and in a free-stream turbulence calibration), the relative error in $\langle u^3 \rangle$ is greater than 2.05, for a signal-to-noise ratio of less than one-half.

This error analysis is not sophisticated enough to represent all errors in estimation of higher-order velocity moments, but it is indicative of the magnitude of the problem of estimating dynamical quantities from imperfect kinematical observations. A more complete analysis must properly account for the many sources of error present in EM measurement systems, both electronic and hydrodynamic.

Acknowledgments. This work was initiated with funding from the NOAA National Office of Sea Grant, grant NA80-AA-D-00077, as part of the Nearshore Sediment Transport Study. Most calibration runs and analyses were completed with funding from the U.S. Army Corps of Engineers, Coastal Engineering Research Center, under contract DACW/2-82-C-0014. Some of D.G.A.'s support came from the Woods Hole Oceanographic Institution's Coastal Research Center. S. T. Bolmer performed many of the calibrations for us and reduced much of the analog data. Abigail Ames Spencer helped in the laboratory calibrations during our initial tests. Pam Barrows typed the report. Mr. Y. Meija of the MIT ship model test facility provided needed expertise in experimental work at his facility. His participation assured smooth operations at MIT. W. D. Spencer performed many of the calibrations, reduced much of the data, and designed some of the experimental hardware.

Woods Hole Oceanographic Institution contribution 5626.

REFERENCES

Achenbach, E., The effects of surface roughness and tunnel blockage on the flow past spheres, *J. Fluid Mech., 65*, 113–125, 1974.

Appell, G. F., Performance of advanced ocean current sensors, Oceans '77, Institute of Electrical and Electronics Engineers, New York, 1977.

Aubrey, D. G., and W. Hill, Performance of bottom-mounted directional wave sensors, Oceans '84, vol. 2, pp. 705–710, Institute of Electrical and Electronics Engineers, New York, 1984.

Aubrey, D. G., W. D. Spencer, and J. H. Trowbridge, Dynamic response of electromagnetic current meters, *Tech. Rep. 84-20*, 150 pp., Woods Hole Oceanogr. Inst., Woods Hole, Mass., 1984.

Bevir, M. K., The theory of induced voltage electromagnetic flow meters, *J. Fluid Mech., 43*, 577–590, 1970.

Bivins, L. E., Turbulence effects on current measurement, M.S. thesis, 104 pp., Univ. of Miami, Coral Gables, Fla., 1975.

Cunningham, P. M., R. T. Guza, and R. L. Lowe, Dynamic calibration of electromagnetic flow meters, Proceedings of Oceans '79, pp. 298–301, Institute of Electrical and Electronics Engineers, New York, 1979.

Cushing, V., Electromagnetic water current meter, Proceedings of Oceans '76, pp. 25C-1 to 25C-17, Institute of Electrical and Electronics Engineers, New York, 1976.

Draper, N. R., and H. Smith, *Applied Regression Analysis*, 407 pp., John Wiley, New York, 1966.

Fernholz, H. H., External flows, in *Turbulence*, edited by P. Bradshaw, 339 pp., Springer-Verlag, New York, 1978.

Griffiths, G., The effect of turbulence on the calibration of electromagnetic current sensors and an approximation of their spatial response, *Rep. 68*, 14 pp., Inst. of Oceanogr. Sci., Wormley, 1979.

Gross, T. F., and A. R. M. Nowell, Mean flow and turbulence scaling in a tidal boundary layer, *Cont. Shelf Res., 2*, 109–126, 1983.

Grosskopf, W. G., D. G. Aubrey, M. G. Mattie, and M. Mathiesen, Field intercomparison of nearshore directional wave sensors, *IEEE J. Oceanogr. Eng., OE-8*, 254–271, 1983.

Heathershaw, A. D., Measurements of turbulence in the Irish Sea Benthic Boundary Layer, in *The Benthic Boundary Layer*, edited by I. N. McCave, pp. 11–31, Plenum, New York, 1976.

McCullough, J. R., Near-surface ocean current sensors: Problems and performance, Proceedings of a working conference on Current Measurement, *Tech. Rep. DEL-SG-3-78*, pp. 9–33, Coll. of Mar. Stud., Univ. of Del., Newark, 1978.

Mei, C. C., *Applied Dynamics of Ocean Surface Waves*, 740 pp., Wiley Interscience, New York, 1983.

Nakamura, Y., and Y. Tomonari, The effects of surface roughness on the flow past circular cylinders at high Reynolds numbers, *J. Fluid Mech., 123*, 363–378, 1982.

Roshko, A., Experiments of the flow past a circular cylinder at very high Reynolds number, *J. Fluid Mech., 10*, 345–356, 1961.

Schlichting, H., *Boundary-Layer Theory*, 6th Ed., 748 pp., McGraw-Hill, New York, 1968.

Seymour, R. J., The nearshore sediment transport study, *J. Waterway Port Coastal Ocean Eng., 109*, 79–85, 1983.

Shercliff, J. A., *The Theory of Electromagnetic Flow Measurement*, Cambridge University Press, New York, 1962.

Smith, J. D., Measurement of turbulence in oceanic boundary layers, Proceedings of a Working Conference on Current Measurement, *Tech. Rep. DEL-SG-3-78*, pp. 95–128, Coll. of Mar. Stud., Univ. of Del., Newark, 1978.

D. G. Aubrey, Woods Hole Oceanographic Institution, Woods Hole, MA 02543.

J. H. Trowbridge, University of Delaware, Newark, DE 19716.

(Received February 25, 1985;
accepted April 7, 1985.)